

Free carrier lifetime modification for silicon waveguide based devices

N.M.Wright^{1*}, D.J.Thomson¹, K.L.Litvinenko¹, W.R.Headley¹, A.J.Smith¹, A.P.Knights², J.H.B.Deane³, F.Y.Gardes¹, G.Z.Mashanovich¹, R.Gwilliam¹, G.T.Reed¹

¹Advanced Technology Institute, University of Surrey, Guildford, GU2 7XH, UK

²Department of Engineering Physics, McMaster University 1280 Main Street West, Hamilton, Ontario, L8S 4L7, Canada

³Department of Mathematics & Statistics, University of Surrey Guildford, GU2 7XH, UK

*Corresponding author: Nicholas.wright@surrey.ac.uk

Abstract: We investigate the effect of silicon ion irradiation on free carrier lifetime in silicon waveguides, and thus its ability to reduce the density of two-photon-absorption (TPA) generated free carriers. Our experimental results show that free carrier lifetime can be reduced significantly by silicon ion implantation. Associated excess optical absorption from the implanted ions can be reduced to an acceptable level if irradiation energy and dose are correctly chosen. Simulations of Raman scattering suggest that net gain can be achieved in certain cases without the need for an integrated diode in reverse bias to remove the photo-generated free carriers.

©2008 Optical Society of America

OCIS codes: (230.7370) Waveguides; (250.3140) Integrated optoelectronic circuits; (250.4480) Optical amplifiers.

References and links

1. H. Rong, R. Jones, A. Liu, O. Cohen, D. Hak, A. Fang, and M. Paniccia, "A continuous-wave Raman silicon laser," *Nature*. **433** 725-728 (2005).
2. R. Claps, V. Raghunathan, D. Dimitropoulos, and B. Jalali, "Influence of nonlinear absorption on Raman amplification in Silicon waveguides," *Opt. Express* **12** 2774-2780 (2004).
3. D. Dimitropoulos, D. R. Solli, R. Claps, O. Boyraz, and B. Jalali, "Noise figure of silicon Raman amplifiers," *J. Lightwave. Tech.* **26** 847-852 (2008).
4. D. Dimitropoulos, S. Fathpour, and B. Jalali, "Limitations of active carrier removal in silicon Raman amplifiers and lasers," *Appl. Phys. Lett.* **87** 261108 1-3 (2005).
5. R. L. Espinola, J. I. Dadap, R. M. Osgood, Jr., S. J. McNab, and Y. A. Vlasov, "Raman amplification in ultrasmall silicon-on-insulator wire waveguides," *Opt. Express* **12** 3713-3718 (2004).
6. D. Dimitropoulos, R. Jhaveri, R. Claps, J. C. S. Woo, and B. Jalali, "Lifetime of photogenerated carriers in silicon-on-insulator rib waveguides," *Appl. Phys. Lett* **86** 071115 1-3 (2005).
7. Y. Liu and H. K. Tsang, "Nonlinear absorption and Raman gain in helium-ion-implanted silicon waveguides," *Opt. Lett.* **31** 1714-1716 (2006).
8. Silvaco International, 4701 Patrick Henry Drive, Bldg 1, Santa Clara, CA 94054, www.silvaco.com.
9. P. J. Foster, J. K. Doylend, P. Mascher, A. P. Knights, and P. G. Coleman, "Optical attenuation in defect-engineered silicon rib waveguides," *J. Appl. Phys.* **99**, 073101 1-7 (2006).
10. M. Waldow, T. Plötzing, M. Gottheil, M. Först, J. Bolten, T. Wahlbrink, and H. Kurz, "25ps all-optical switching in oxygen implanted silicon-on-insulator microring resonator," *Opt. Express* **16**, 7693-7702 (2008)
11. M. Y. Shen, C. H. Crouch, J. E. Carey, R. Younkin, E. Mazur, M. Sheehy, and C. M. Friend, "Formation of regular arrays of silicon microspikes by femtosecond laser irradiation through a mask," *Appl. Phys. Lett.* **82** 1715-1717 (2003)
12. A. Liu, H. Rong, R. Jones, O. Cohen, D. Hak, and M. Paniccia, "Optical amplification and lasing by stimulating raman scattering in silicon waveguides," *J. Lightwave. Tech.* **24**, 1440-1455, 2006
13. OriginLab Corporation, One Roundhouse Plaza, Suite 303, Northampton, MA 01060, USA, www.originlab.com.

1. Introduction

The Raman effect has been used successfully to produce a silicon laser [1], however very high intensity pump lasers are required to generate amplification due to a non-linear effect known as two-photon-absorption (TPA) [2] which causes free-carrier absorption (FCA) loss that can exceed Raman gain as well as depleting pump photons. Integrated p-i-n diodes have been used previously to remove these carriers, and hence reduce the effective carrier lifetime. However they appear less effective at high powers due to carrier screening of the reverse bias voltage [3, 4]. Scaling the waveguide to sub-micrometer sized dimensions can reduce the effective lifetime of carriers due to enhanced surface recombination [5, 6], however in that case the problem of high coupling losses has to be addressed.

It has already been shown that implanting helium into rib waveguides [7] can reduce the carrier lifetime without a drastic increase in propagation loss. A net Raman gain of 0.065dB was measured in that case without the need for a reverse bias diode to remove the photo-generated free carriers.

The work in this paper is based on the implantation of silicon. We discuss the use of ion induced defects to trap the carriers generated from the TPA process, and the effect of the implanted defects on propagation inside the waveguide. The depth of the defects in the waveguide and their concentration is varied to investigate the effect this has on free carrier lifetime and excess optical absorption. Modelling has shown that high gain is possible for a device not containing an electric field, if a low effective carrier lifetime can be achieved with no increase in propagation loss [3]. Here we show that the introduction of a thin defect layer at the waveguide surface produces this scenario.

Silicon ion implantation is a process now used commonly in the fabrication of CMOS type devices, for example in the creation of shallow amorphous layers. Further use of such self ion implantation prevents any possibilities of modification via chemical doping effects. Previous studies of defects created via self irradiation of silicon are substantial in volume and thus significant data is available to those wishing to model the recombination characteristics of defect engineered structures.

2. Experimental method and results

Silicon rib waveguides were fabricated on a (100) silicon-on-insulator (SOI) wafer. The rib dimensions were nominally width $1\mu\text{m}$ and height $1.35\mu\text{m}$. The waveguides had a length of $8000\mu\text{m}$.

Ion implantation modeling was carried out using ATHENA [8] to find the damage range in relation to the rib waveguide cross sectional dimensions. Ion implantation energies were chosen to provide a range of damage depths in the rib waveguide. This varied from near-surface implantation range to fully implanted waveguides.

Measurement of propagation loss was made in a manner similar to that employed by Foster et al. using a broadband source with a wavelength range of 1530nm to 1610nm [9]. Implant windows varied in length from $0\mu\text{m}$ to $8000\mu\text{m}$ increasing in steps of either $1000\mu\text{m}$ or $2000\mu\text{m}$. Table 1 summarizes the range of energy and dose of the silicon implantations used in our experiments, the associated excess propagation loss in dB/cm is also shown. The loss was measured on 12 occasions for each waveguide. The values reported in Table 1 are the mean of those measurements. The waveguide loss before implantation was $\sim 1\text{-}2\text{dB/cm}$.

Table 1. Ion induced excess propagation loss in dB/cm for associated energy and dose implants

<i>Energy keV</i>	<i>Dose cm⁻²</i>				
	$1 \times 10^{10} \text{cm}^{-2}$	$1 \times 10^{11} \text{cm}^{-2}$	$5 \times 10^{11} \text{cm}^{-2}$	$1 \times 10^{12} \text{cm}^{-2}$	$1 \times 10^{13} \text{cm}^{-2}$
400	n/a	0.19 ± 0.02	0.25 ± 0.03	0.54 ± 0.07	n/a
750	0.24 ± 0.02	1.38 ± 0.06	6.56 ± 0.17	11.56 ± 0.20	78.02 ± 0.99
1150	0.55 ± 0.09	4.11 ± 0.05	22.38 ± 0.14	35.59 ± 0.19	167.39 ± 1.5
1575	1.91 ± 0.04	4.62 ± 0.05	27.50 ± 0.36	53.18 ± 0.47	n/a
2000	1.61 ± 0.17	4.99 ± 0.04	25.14 ± 0.25	38.94 ± 0.47	171.94 ± 1.1

Figure 1 shows excess loss introduced by ion implantation versus dose, for different implantation energies. As dose increases, so does the excess loss introduced to the waveguide. Excess loss also increases with implantation energy (for a given dose), until the highest energy of 2000keV, at which point the peak of the asymmetric damage profile passes through the SOI device and is positioned in the buried oxide below.

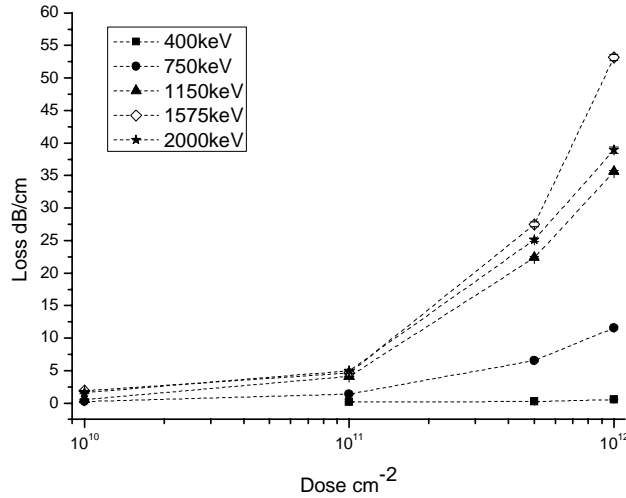


Fig. 1. Experimental data of excess loss versus dose for different silicon implantation energies

The experimental setup for carrier lifetime measurements required the addition of a femto-second pulsed laser directed onto the top of the waveguide. Figure 2 shows a diagram of the measurement technique. The broadband source used previously to measure propagation loss, is now used as the probe beam in this experiment, with a maximum power available of ~4mW. The pump beam had a pulse width ~80fs.

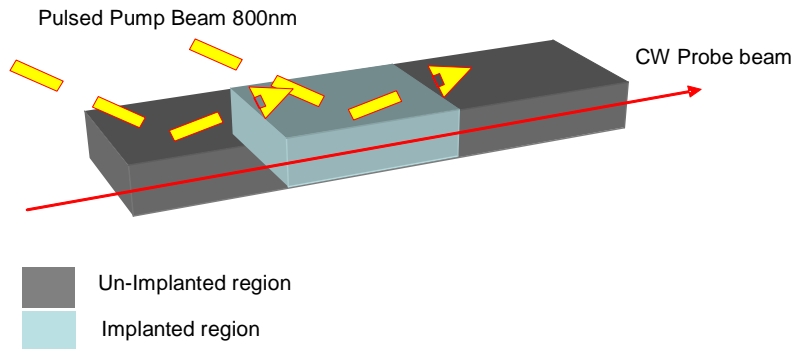


Fig. 2. Free carrier lifetime measurement technique. The laser is aligned with the top of the waveguide. This excites carriers which attenuate the broadband beam. During the off-cycle of the pump the carriers recombine.

Directing the pump beam from above onto the waveguide being measured, allowed both implanted and un-implanted regions to be measured using near identical experimental conditions. This approach is similar to the one used by Waldow et. al, to investigate argon and oxygen implantation on switching speeds in silicon microring resonators [10]. The penetration depth with a wavelength of 800nm in silicon is much larger than the waveguide

height in this experiment [11]; hence a distribution of carriers will exist throughout the waveguide which will behave in the same manner as those generated by the co-linear approach [12].

The generation and exponential recovery of carriers was displayed on a digital oscilloscope via a 12GHz bandwidth fibre coupled detector. A typical trace is shown in Fig. 3; this was for a 400keV $1 \times 10^{12} \text{cm}^{-2}$ dose. Originlab [13], a commercial data analysis and graphing tool, was used to calculate the free carrier lifetime from the exponential decay of the waveform.

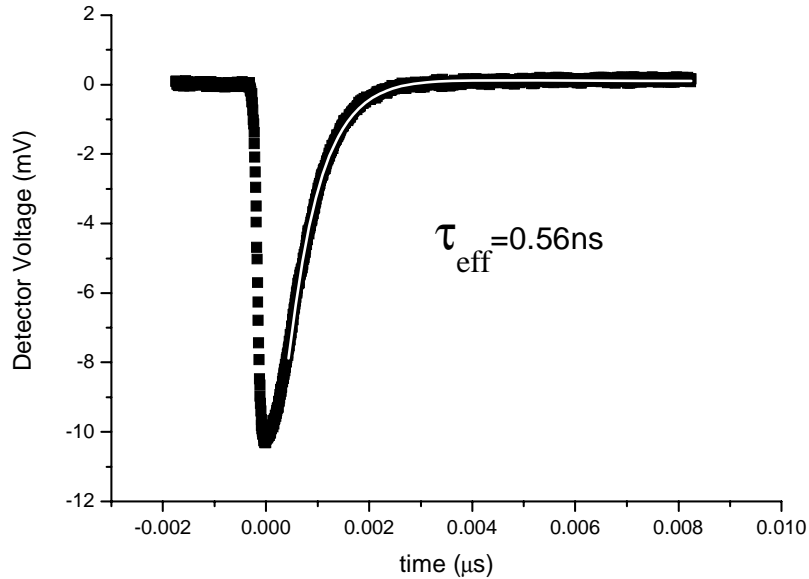


Fig. 3. Time dependence of the transmitted probe signal in a 400keV $1 \times 10^{12} \text{cm}^{-2}$ implanted silicon waveguide excited by a femto-second pump pulse. The probe signal decreases as the pump pulse excites carriers. During the off cycle, the probe signal recovers due to recombination of carriers. Fitting the data with an exponential curve (solid line) gives a decay time of 0.56ns

Table 2 summarizes the percentage reduction in free carrier lifetime caused by the various silicon ion irradiations. The average un-implanted free carrier lifetime was $\sim 4 \text{ns}$.

Table 2. Percentage reduction in free carrier lifetime for labeled silicon ion dose and energy

Energy keV	Dose cm^{-2}			
	$1 \times 10^{10} \text{cm}^{-2}$	$1 \times 10^{11} \text{cm}^{-2}$	$5 \times 10^{11} \text{cm}^{-2}$	$1 \times 10^{12} \text{cm}^{-2}$
400	n/a	72.5	79.5	85.4
750	71.27	86.15	93.74	94.021
1150	56.22	86.55	94.47	
1575	55.011	88.15		
2000	52.171	88.46		

The largest reduction in lifetime was 94.47%; corresponding to a carrier lifetime of 0.23ns. However the excess loss introduced into the waveguide for this implantation was unacceptably high $\sim 22.38 \text{dB/cm}$. In comparison, utilizing the lowest ion implantation energy yields an 85.4% reduction in lifetime corresponding to $\sim 0.56 \text{ns}$, for only $\sim 0.54 \text{dB/cm}$ excess loss. Figure 4 displays excess loss data for the 400keV implantation together with the percentage reduction in free carrier lifetime, as a function of ion dose. The carrier lifetime for each corresponding dose is also shown.

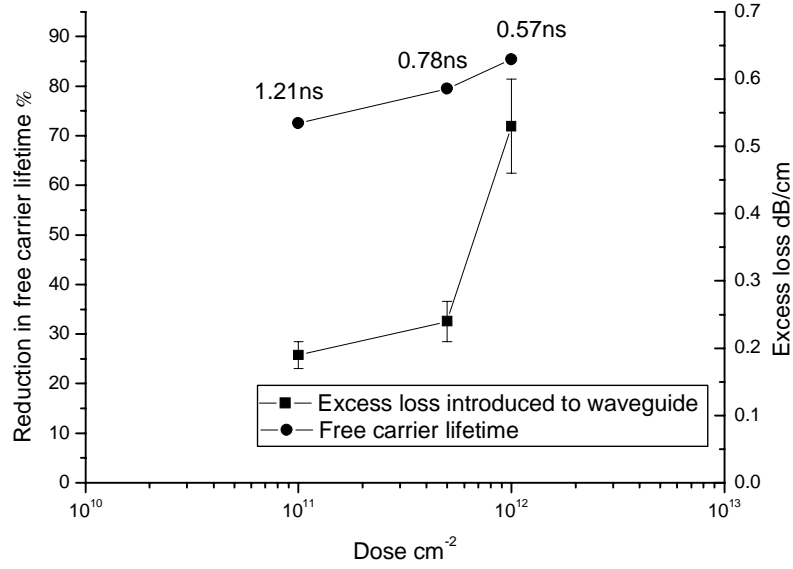


Fig. 4. Plot comparing excess loss and reduction in free carrier lifetime for 400keV energy with 10^{11} , 5×10^{11} and 10^{12}cm^{-2} doses. As the concentration (ion implantation dose) of defects increases so does the excess loss and reduction in free carrier lifetime.

3. Raman simulation

Assuming a low loss waveguide and knowing the excess loss and free carrier lifetime effects for various ion implantation energies and doses, the net Raman gain can be calculated using the approach of Liu et al.[12]. Taking into account TPA and TPA induced FCA, the optical power $P(z)$ evolution along the waveguide is given by Eq. (1) [12]:

$$\frac{dP(z)}{dz} = -\alpha P(z) - \frac{\beta}{A_{eff}} P^2(z) - \sigma N(z)P(z) \quad (1)$$

where α is the linear absorption of the waveguide with the addition of the excess loss value for the chosen energy and dose implant, σ is the FCA cross section, β is the TPA coefficient, A_{eff} is the effective area of the mode and $N(z)$ is the free carrier density. For a continuous wave regime, the carrier density in the waveguide is given by Eq. (2):

$$N(z) = \frac{\beta \lambda_P \tau_{eff} P^2(z)}{2hcA_{eff}^2} \quad (2)$$

Knowing the pump power $P(z)$, the probe power (Stokes power), $P_s(z)$ can be calculated using Eq. (3)

$$\frac{dP_s(z)}{dz} = -\alpha P_s(z) - \frac{2\beta - g_r}{A_{eff}} P(z)P_s(z) - \sigma_s N(z)P_s(z) \quad (3)$$

where g_r is the Raman gain coefficient.

Numerically solving Eq. (3) using the pump power obtained from Eq. (1) for a probe input power $P_s(0)$ as an initial condition, the net gain of the waveguide can be obtained using Eq. (4), where $P_s(L)$ is the probe output power obtained from Eq. (3), and L is the waveguide length.

$$G = 10 \log \frac{P_s(L)}{P_s(0)} \quad (4)$$

Figure 5 shows the optical net continuous wave Raman gain as a function of input pump power in a 4.8cm silicon waveguide for $1 \times 10^{11} \text{cm}^{-2}$, $5 \times 10^{11} \text{cm}^{-2}$ and $1 \times 10^{12} \text{cm}^{-2}$ silicon doses at 400 keV. The following values were used in the modelling, taken from Liu et al [12]:- $\alpha = 0.2 \text{dB/cm}$, $\beta = 0.5 \text{cm/GW}$, $\sigma = 1.45 \times 10^{-17} \text{cm}^2$, $\sigma_s = 1.71 \times 10^{-17} \text{cm}^2$, $A_{\text{eff}} = 1.5 \mu\text{m}^2$, $\lambda_{\text{pump}} = 1550 \text{nm}$, $\lambda_{\text{stokes}} = 1684 \text{nm}$, $g_r = 9.5 \text{cm/GW}$. That group reported that a value of $g_r = 9.5 \text{cm/GW}$ gave good agreement between theoretical and experimental results. They also noted that there are differing values for the TPA coefficient, which may require further investigation.

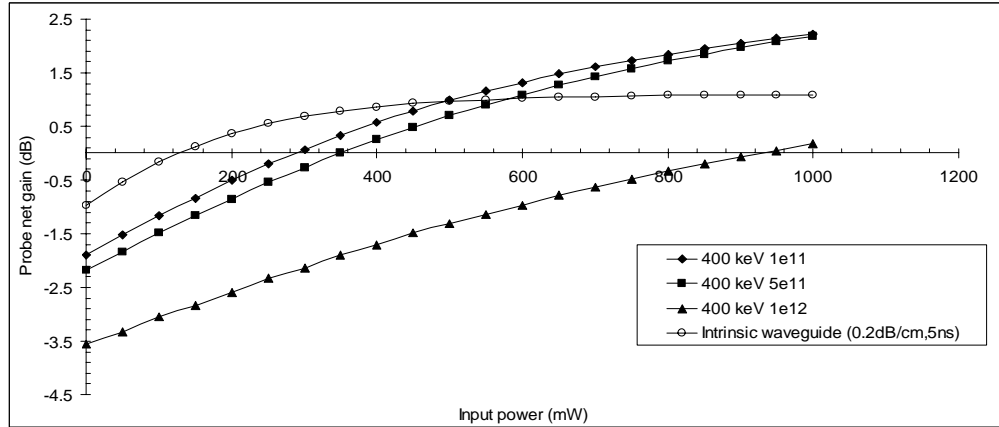


Fig. 5. Modeled optical net continuous wave Raman gain as a function of input pump power in a 4.8cm silicon waveguide for $1 \times 10^{11} \text{cm}^{-2}$, $5 \times 10^{11} \text{cm}^{-2}$ and $1 \times 10^{12} \text{cm}^{-2}$ 400 keV silicon doses.

In defect engineered waveguides the most important factor in determining net Raman gain is the tradeoff between lifetime reduction and linear loss. For example, in Fig. 5 the lower ion implantation doses result in the highest Raman gain, even though the lifetime reduction is not as small as for the highest dose. The intrinsic waveguide produces the highest net gain up to $\sim 450 \text{mW}$ since it has the lowest linear loss; however TPA generated FCA dominates as the pump power is increased resulting in the $5 \times 10^{11} \text{cm}^{-2}$ dose producing the highest gain for 1W.

4. Summary

This work has shown that silicon ion implantation is successful at reducing the free carrier lifetime of a silicon waveguide. Low energy silicon implantation provides the best compromise between excess linear loss and reduction in free carrier lifetime, due to little or even zero modal overlap between the damage and the propagating signal. Simulations show that Raman gain is possible in these waveguides, however low loss propagation, of the order of 0.2dB/cm is required. It should be noted that the procedure of implantation to modify carrier lifetime would be best utilized as a back end process due to the fact that damage introduced by low dose Si ions, anneals out at $\sim 350^\circ \text{C}$ [9]. It should be noted however, that this is also true for any low dose ion implantation process such as those discussed for other ion species.

Acknowledgments

This work has been partly funded by the Engineering and Physical Sciences Research Council (EPSRC) programme, "UK Silicon Photonics", partly by the European Union framework 6 program, "Circles of light" and partly by an EPSRC studentship.